Journal of Thermal Biology 140 (2026) 104531

Contents lists available at ScienceDirect

Journal of Thermal Biology

journal homepage: www.elsevier.com/locate/jtherbio

Upper thermal tolerance of the euryhaline fish *Fundulus heteroclitus* is lower in freshwater and shaped by environmental salinity–acclimation time interaction

André Barany [a,b,c,*,1], Anyell Caderno [c,1], Paula Simó-Mirabet [c], Ciarán Alvar Shaughnessy [d], Juan Antonio Martos-Sitcha [c], Juan Miguel Mancera [c], Stephen Daniel McCormick [b]

[a] Departamento de Genética, Fisiología y Microbiología, Facultad de Ciencias Biológicas, Universidad Complutense de Madrid, Madrid, CAM, 28040, Spain
[b] Department of Biology, Morrill Science Center, University of Massachusetts, Amherst, MA, 01003, United States
[c] Departamento de Biología, Facultad de Ciencias del Mar y Ambientales, Universidad de Cádiz, Puerto Real, Cádiz, AND, 11519, Spain
[d] Department of Biology, Oklahoma State University, Stillwater, OK, 74078, United States

ARTICLE INFO

Keywords:
Climate change
Critical thermal maximum
Killifish
Osmoregulation
Salinity
Temperature

ABSTRACT

This study investigates whether salinity affects the upper thermal tolerance (CT_{max}) of the euryhaline mummichog (*Fundulus heteroclitus*). Mummichogs were acclimated to seawater (38 ppt, SW) or freshwater (<1 ppt, FW) at 18.5°C (T_{acc}), then transferred to the opposite salinity. CT_{max} and physiological profiles were assessed on days 0, 1, 3, 6, and 13 post-transfer. CT_{max} was consistently lower in FW than in SW, regardless of prior acclimation. Compared to the T_{acc} controls, CT_{max} exposure reduced plasma ion levels in FW-transferred fish and increased them in SW-transferred fish. In both salinities, CT_{max} exposure raised plasma cortisol, glucose, lactate, and hematocrit.

Second-order Akaike Information Criterion (AICc) modeling identified the Salinity/Acclimation time interaction as the most parsimonious predictor of CT_{max}. Furthermore, multivariate analysis reveals that potential underlying mechanisms of thermal shock diverged by environment. In FW, CT_{max} progressively declined over time, constrained by a direct metabolic tax—the recruitment of high-overhead, residual (ouabain-insensitive) ATPase activity required to maintain ionic stability—alongside a unique stress-erythropoiesis response. Conversely, in SW, thermal performance improved over time and was tightly coupled to osmolality, glucose and cortisol. Additionally, lactate accumulation was a shared response across salinities. We conclude that the synergy of ion-poor environments and rising temperatures creates a unique performance trade-off that imposes a permanent thermal penalty, potentially increasing the climate vulnerability of estuarine populations beyond current ecological forecasts.

1. Introduction

Climate change is predicted to influence water temperature (Venegas et al., 2023), salinity (Feist et al., 2025), and ocean acidification (Garcia-Soto et al., 2021; Leung et al., 2022), with potential widespread impacts on the distribution of aquatic organisms. Describing the physiological factors that determine the tolerance of aquatic organisms to shifts in these environmental conditions will help identify the ecological implications of climate change.

One commonly examined quantitative metric of thermal tolerance in aquatic organisms is critical thermal maxima (CT_{max}). A number of environmental factors have been shown to influence thermal tolerance in aquatic organisms (Ern et al., 2023), including temperature (Sandersfeld et al., 2015, 2017; Stewart et al., 2023), photoperiod, daily (Bulger and Tremaine, 1985) and seasonal rhythms (Hines et al., 2019), oxygen availability (Andreassen et al., 2022), reproductive status (Mugwanya et al., 2022), ontogeny (Dahlke et al., 2020), behavior (Christensen et al., 2021; Kochhann et al., 2021), body size (Kraskura et al., 2023) and salinity (Metzger et al., 2016; Comte and Olden, 2017; Shaughnessy and McCormick, 2018; Hines et al., 2019).

* Corresponding author. Departamento de Genética, Fisiología y Microbiología, Facultad de Ciencias Biológicas, Universidad Complutense de Madrid, 28040, Madrid, CAM, Spain.
E-mail address: abarany@ucm.es (A. Barany).
[1] These authors contributed equally to this work.

https://doi.org/10.1016/j.jtherbio.2026.104531
Received 12 August 2025; Received in revised form 24 May 2026; Accepted 30 June 2026
Available online 11 July 2026
0306-4565/© 2026 The Authors. Published by Elsevier Ltd. This is an open access article under the CC BY license (http://creativecommons.org/licenses/by/4.0/).

Salinity is a major ecological barrier for fish, with the vast majority of fish restricted to either freshwater (FW) or seawater (SW) and only about 4% able to move between the two delimited environments (Schultz and McCormick, 2012). Salinity change requires adaptive responses in osmoregulatory organs, including the gills, gut, and kidney, in order to maintain internal osmoregulatory homeostasis (Marshall and Grosell, 2006), and climate change is expected to significantly alter salinity patterns in aquatic ecosystems. Moreover, increased sea level rise will extend the reach of high saline waters throughout estuaries and into FW systems, and melting glaciers and ice sheets will reduce overall ocean salinity (Röthig et al., 2023).

Many studies have assessed the upper thermal tolerance in fishes. However, these studies predominantly examine thermal tolerance of fish under constant salinity conditions, whether it be FW (Barrionuevo and Femandes, 1995; Elliott and Elliott, 1995; Currie et al., 1998; Zaragoza et al., 2008; Zhang and Kieffer, 2014), or SW (Tsuchida, 1995; Fangue et al., 2006; Murchie et al., 2011; Healy and Schulte, 2012a, 2012b; Madeira et al., 2013). Far fewer studies have examined the thermal tolerance in fish during the process of salinity acclimation (Metzger et al., 2016; Vargas-Chacoff et al., 2018;Shaughnessy and McCormick, 2018; Hines et al., 2019; Hieu et al., 2021). Broadly, there is little consensus on how salinity influences thermal limits: some report clear effects (Chen and Chen, 1999; Jian et al., 2003; Sardella et al., 2008; Sardella et al., 2008; Cheng et al., 2013; Metzger et al., 2016; Shaughnessy and McCormick, 2018), whereas others find none (Haney and Walsh, 2003; Denisse Re et al., 2006, 2012). Variation in the impact of salinity on thermal tolerance between species may be expected, considering the wide range of physiological and behavioral responses of fishes to osmoregulatory and thermal stressors (Evans and Kültz, 2020; Hall-Scharf et al., 2025; Monette et al., 2025). Some of the observed variations may also arise from differences in experimental approaches, including that many studies examine only fish fully acclimated to FW or SW, but do not examine changes in thermal tolerance during transition between different salinities.

The mummichog (*Fundulus heteroclitus*) inhabits temperate tidal marshes that are characterized by wide variations in salinity and temperature. Its euryhaline and eurythermal characteristics have made it a widely used model species for studies on both osmoregulation and thermal tolerance. In this study we tested how salinity affects CT_{max} by measuring a focused set of physiological variables expected to influence osmotic balance and metabolic stress — plasma cortisol, osmolality, chloride, glucose, lactate, triglycerides, hematocrit, gill Na^+/K^+-ATPase (NKA) activity, and body mass. We measured CT_{max} in a time-course during transfers between FW and SW (days 0, 1, 3, 6, 13) and sampled the same physiological variables at the end of the CT_{max} exposure. Our aim was twofold: (1) to describe how these parameters respond to salinity change, and (2) to test which environmental or physiological factors, or their interactions, explain variation in CT_{max}.

2. Materials and methods

2.1. Experimental animals and holding conditions

A total of 362 mummichog (mass: 6.32 ± 0.01 g) of mixed sex were used in this study. Fish were collected from the marshes of Puerto Real (Cádiz Bay, Spain) and transported to the University of Cádiz fish facility. For each salinity-transfer experiment (SW→FW and FW→SW), 10–11 fish per treatment per day were sampled. At each time point (days 0, 1, 3, 6, and 13), fish were assigned to either T_{acc} controls or CT_{max}-tested individuals, yielding 20–22 fish per salinity per day. To maintain consistent handling and avoid overloading daily CT_{max} testing, the two salinity-transfer experiments were run on alternating schedules. In total, this design produced 182 CT_{max} trials and 180 control samples, corresponding to all 362 fish. This population was first detected in the 1970's on the Southwestern coast of Spain, assuming that due to an anthropogenic introduction, and is likely ancestrally related to populations in eastern North America (Bernardi et al., 1995; Morim et al., 2019). Prior to experimentation, fish were held in two flow-through (~10 L min^{-1}) 200 L tanks supplied with aeration, maintained at 18°C (T_{acc}) and natural photoperiod (October to November; latitude 36° 31′ 34″ N) with either SW (38 ppt) or FW (<1 ppt; dechlorinated municipal water) for at least 4 weeks. Fish were fed commercial aquaculture feed (1 mm, Gilthead Seabream Perla, Skretting, Spain) at 2% of body mass twice daily, and feed was withheld for 24 h before sampling and CT_{max} testing. Water changes of one-third of the tank volume were performed daily. No notable mortality was recorded during either the acclimation phase or the experimental procedure. All fish appeared in good health and exhibited normal behavior throughout experimentation, except in the final moments of CT_{max} testing, when the fish lost equilibrium.

2.2. Salinity acclimation trials

Prior to salinity change (day 0), fish had been held and long-term acclimated to either SW or FW (hereafter acclimation experimental tanks at T_{acc}); on day 0 they were directly transferred to the opposite salinity (SW→FW or FW→SW). To ensure that handling did not influence the analyses, control fish not subjected to a salinity switch were net-transferred into a new acclimation experimental tank of identical salinity. These handling controls were run in parallel with the transferred fish, and for every sampling day, salinity (FW and SW), and condition (T_{acc} and CT_{max}), each treatment had a matched control group that experienced the same handling but remained in its original acclimated salinity. CT_{max} was assessed and tissue sampling was performed on days 0 (prior to salinity transfer, serving as baseline CT_{max} controls for fully acclimated FW and SW fish), 1, 3, 6, and 13 post-transfer. On each day, tissues were obtained from fish at T_{acc} and from fish immediately upon losing equilibrium at CT_{max}.

2.3. CT_{max} trials

CT_{max} trials took place in 6.7 L glass aquaria tanks (hereafter CT_{max} tanks) with water conditions (i.e., salinity and temperature) identical to salinity acclimation experimental tanks. Each CT_{max} tank was equipped with two air stones to ensure proper circulation and aeration, maintaining oxygen levels above 80% saturation. Prior to the CT_{max} trials, fish were netted from salinity acclimation experimental tanks to CT_{max} trial tanks and allowed to acclimate for 1 h.

To assess the CT_{max}, heated water (50°C) from a header tank was added to the center of the CT_{max} trial tanks at a flow rate of 50-100 mL per minute to achieve the desired warming rate, using the same FW or SW source of water as the corresponding treatment. At the beginning of the CT_{max} trial, temperature was progressively raised from 18°C (T_{acc}) at a rate of 10°C per hour, until reaching 30°C within the first hour. Subsequently, the rate of temperature increase was adjusted to 5°C per hour for the remainder of the test. No more than a 0.1°C difference was detected across CT_{max} trial tank replicates. Fish were continuously monitored for signs of reaching their upper thermal limit, which was defined as a rapid, erratic burst of swimming that fish display as they approach their upper thermal limit ('shooting') lasting 3-5 s and/or the loss of equilibrium (LOE) (Becker and Genoway, 1979). Preliminary observations indicated that the shooting behavior was quickly followed by LOE and death. In both endpoint scenarios, either shooting or LOE, fish were no longer responsive to the presence of a net in the tank, and CT_{max} was not observed to be influenced by the behavior of other fish or by the removal of fish within the tank; Immediately after reaching CT_{max}, fish were transferred into anesthetic at the same temperature to prevent recovery or further stress, and tissue samples were collected as described in subsection 2.4.

2.4. Sampling protocol

At all sampling points, fish were sampled from salinity trial tanks just

before CT_{max} tests were initiated and from CT_{max} tanks immediately after LOE. Fish were netted and euthanized with a high dose of 2-phenoxyethanol (1 mL L^{-1} in water of their respective salinity), weighed, and sampled for blood within 5 min of the initial removal from the tank. Blood was collected from the caudal vessels into 0.5-mm heparinized capillary tubes after the caudal peduncle was severed. The blood samples were then centrifuged at 4000 g for 3 min at 4°C, and hematocrit values were immediately determined before centrifugation, using a microhematocrit reader as the percentage of total blood volume. Plasma was then snap-frozen in liquid nitrogen. The second-gill arch from each side was excised, and a small portion consisting of a few gill filaments was placed in 100 μL of ice-cold sucrose-EDTA-imidazole (SEI) buffer (150 mM sucrose, 10 mM EDTA, 50 mM imidazole, pH 7.3) and frozen for later analysis of ATPase activity. All other biological tissues (plasma and gill) were immediately frozen and stored at −80°C until further analysis.

2.5. Tissue analysis

All colorimetric endpoint and kinetic assays were run on an Automated Microplate Reader (PowerWave 340, BioTek Instrument Inc., Winooski, VT, USA) using KCjunior™ software. Cortisol levels were analyzed using a commercial enzyme immunoassay kit (Arbor Assays, Cortisol K003-H5, Ann Arbor, MI, USA). Plasma metabolite concentrations (glucose, lactate, and triglycerides) and chloride were determined using commercial colorimetric kits from Spinreact (Barcelona, Spain; Glucose-HK Ref. 1001200; Lactate Ref. 1001330; Triglycerides (TAG) Ref. 1001311; and Chloride Ref. 1001360) with reactions adapted to 96-well microplates. All standards were run in duplicate, while samples were measured in single replicates due to limitations in plasma volume. Osmolality was measured in 8 μL plasma samples using a Fiske One-Ten vapor pressure osmometer (Fiske Associates, Advanced Instruments, Norwood, MA, USA).

Gill NKA activity was analyzed using 96-well microplates run at 25°C for 10 min, as described by McCormick (1993). In short, frozen tissues were homogenized on ice in 150 μL of SEID (0.1% sodium deoxycholate in SEI buffer, pH 7.3) and centrifuged at 3,200g for 5 min at 4°C. The supernatant was assayed in duplicate for ATPase activity in the presence and absence of the NKA-specific inhibitor ouabain (0.5 mM). The difference between the inhibited and uninhibited solutions was used to calculate NKA-specific (ouabain-sensitive) and residual ATPase activity (both expressed as μmol·ADP mg $protein^{-1}·h^{-1}$). Total protein was measured to normalize ATPase activity across samples using the bicinchoninic acid protein assay with bovine serum albumin standard (Thermo Scientific, Rockford, IL, USA).

2.6. Statistical analysis

2.6.1. Dataset management and experimental design

A dual-modeling approach was employed to characterize the physiological response. For traditional group comparisons (ANOVA), parallel control groups were treated as independent temporal references for each sampling point (Dataset *Raw_Data* file provided in the supplementary files). In contrast, for systems-level analyses (AICc-based GLMs, Pearson correlations and multiple linear regressions), these controls were pooled and assigned to "Day 13″ cohort. This categorization reflects their stable, long-term acclimation status (13 days or ≥ 4 weeks), fulfilling the standard requirement for physiological stabilization in euryhaline species (Marshall et al., 1999) and anchoring the models to a biologically relevant acclimation plateau (Dataset *AIC.CTmax,* derived from the *Raw_Data* file provided in the supplementary files).

2.6.2. Univariate and multivariate modeling

All statistical analyses were performed using GraphPad Prism (version 10.4.1), and R (v.4.3.2) with statistical significance set at $P \leq 0.05$. Shapiro-Wilk and Bartlett tests confirmed both normality and equal variance of the data. Outliers were identified and removed using the ROUT method (Robust regression and Outlier removal, Q = 1%), which applies robust nonlinear regression, tests residuals with a False Discovery Rate approach, and then performs ordinary least-squares regression on the remaining data; the coefficient Q defines the stringency of detection, limiting the false discovery rate to approximately 1% (Motulsky and Brown, 2006). If ANOVA requirements were not met, a natural log, square root or exponential transformation was performed to correct for homoscedasticity or non-normality among residuals (chloride, glucose, lactate, and TAG). Several transformations of cortisol data and the use of ranks were unable to result in normality and equal variance. Thus, untransformed cortisol data were used in ANOVAs. When two-way ANOVA (factors: salinity and time) yielded significant differences, Sidak's *post hoc* test was used to identify significantly different groups. All figures depict untransformed data. Additionally, three-way ANOVA analyses were conducted to support the evaluation of salinity (S), time post-transference (t), and thermal stress (CT_{max}), as well as their interactions (×) across all studied physiological parameters in mummichog during either SW to FW (Supplementary Results SR1; Supplementary Table S1) or FW to SW transition (Supplementary Results SR2; Supplementary Table S2).

To identify the primary drivers of thermal tolerance (CT_{max}), we constructed Generalized Linear Models (GLMs) using a Gaussian distribution and identity link function (Table 1 and Supplementary Table S3). Predictors included salinity, acclimation day, and physiological parameters (excluding mass, see below), incorporating both additive (+) and interactive (×) terms. Note that when variables are combined (+), both are independent, but when they interact (×) they might modify each other. Model selection was performed across 121 candidates using the AICc via the *AICcmodavg* package in R Studio (Table 1). To ensure uniformity across experimental cohorts, body mass was evaluated using a two-way ANOVA (factors: salinity and time). Upon detecting significant interaction between factors ($F_{3,172} = 18.31$, $P < 0.0001$), that indicated a size bias across treatments, body mass was included as a covariate in the top candidate model set. Specifically, the best-fitting model (Salinity × Day + Mass) was utilized for frequentist inference via a Type III Analysis of Covariance (ANCOVA). This approach (implemented via the *drop1* function in R) allowed us to isolate the true physiological effect of salinity and time while mathematically standardizing for the influence of body mass (Significance was set $P < 0.05$). Subsequent model selection via Second-order Akaike Information Criterion (AICc) confirmed that including mass as a covariate, alongside the Salinity × Day interaction, provided the most parsimonious explanation of individual observed thermal tolerance across salinities (Table 2). Following the framework of Burnham and Anderson (2002), AICc was employed instead of Akaike Information Criterion (AIC) because our sample-size-to-parameter ratio was below the recommended threshold for large-sample approximations (n/K > 40 *vs.* n/K = 27.6, in our case of study n = 138 and K = 5), thereby providing a necessary and rigorous bias correction against over-parameterization.

This set of multivariate analysis was conducted for hypothesis generation, exploration comparison, and subsequent AICc-based model selection (Table 1; Table 2). The model selection results provided overwhelming support for the Salinity × Day interaction as the primary driver CT_{max}, which outperformed the next best candidate model by a ΔICc of 343.05 (ΔICcWt = 99.99%). Although minor deviations from normality and homocedasticity were observed in the final GLM, the Gaussian framework was maintained given the robust sample size (n = 138) and the stability of parameter estimates under the Central Limit Theorem (Kwak and Kim, 2017).

To identify coordinated physiological responses, Pearson correlation matrices and heatmaps were generated separately for the SW-to-FW (Fig. 4A) and FW-to-SW (Fig. 4B) direct transference (*corrplot* in R). Additionally pairwise Pearson correlation coefficients (*r*) were calculated separately for FW and SW groups using pairwise complete observations. Statistical significance of each *r* was assessed with a two-tailed *t*-

Table 1
Second-order Akaike Information Criterion (AICc) results of individual physiological parameters of mummichog sampled at CT_{max} after direct transfer from either SW to FW, or SW to FW, to predict observed individual CT_{max}. In this system-level analysis, fish acclimated to their native salinity for ≥4 weeks were integrated into the Day 13 cohort to represent the stable physiological plateau reached at the conclusion of the acclimation trajectory (*AIC.CTmax* file provided in the supplementary files).

Predictors	K	ΔICc	ΔΔICc	ΔICcWt	Cum.Wt	LL	R^2
Sal × Day	5	343.05	0.00	99.99	99.99	−166.29	0.599
Sal + Lac	4	369.50	26.44	0.00	99.99	−180.59	0.507
Sal × Lac	5	371.51	28.45	0.00	100.00	−180.52	0.507
Cl + Lac	4	396.77	53.71	0.00	100.00	−194.23	0.399
Cl × Lac	5	396.93	53.88	0.00	100.00	−193.24	0.408

Columns are defined as follows: K, number of parameters in the model; ΔICc, model score where lower values indicate a better fit; ΔΔICc, difference in ΔICc score from best fitting-model in the set; ΔICcWt, probability that a specific model is the most parsimonious in the candidate set; CumWt, cumulative ΔICcWt represents the probability that a specific model is the most parsimonious among the set of models tested; LL, Log-likelihood, a measure of how well the model parameters explain the observed data; and R^2, a measure of the proportion of the total variation in the dependent variable (i.e., CT_{max}) that is explained by the independent variables included in that specific model. Abbreviations: Sal: salinity; Day: acclimation day; Lac: plasma lactate; Cl: chloride; (+): combinations; and (×): interactions.

Table 2
Analysis of Covariance (ANCOVA) of the effects of salinity and acclimation day on the critical thermal maximum CT_{max} of mummichog, with body mass included as a covariate. The row labeled "Mass + Sal × Day" represents the complete model and serves as the reference for model comparisons.

Model	Df	Sum of Sq	RSS	AICc	F value	Pr(<F)
Mass + Sal × Day	NA	NA	107.065	−75.514	NA	NA
Mass	1	5.010	112.074	−69.283	8.001	0.005**
Sal	1	5.233	112.298	−68.924	8.359	0.004**
Day	3	4.429	111.493	−74.218	2.358	0.073
Sal × Day	3	45.556	152.621	−17.700	24.253	$3.98x10^{-13}$****

Columns are defined as follows: Df (Degrees of Freedom) indicates the number of independent values used in the calculation; Sum of Sq (Sum of Squares) represents the marginal variation attributed to each specific term; RSS (Residual Sum of Squares) and AICc (Second-order Akaike Information Criterion) indicate the model's fit and parsimony if that specific term were removed; the F-value is the test statistic for the effect; and Pr(>F) is the associated P-value **P ≤ 0.01; ****P ≤ 0.0001); NA: Not applicable. Further details are in legend footnote Table 1.

test ($t = r\sqrt{n-2}/\sqrt{1-r^2}$, with $n-2$ degrees of freedom) testing H_0: ρ = 0 and indicated on the matrix with asterisks (*$P < 0.05$, **$P < 0.01$, ***$P < 0.001$). Cell color reflects the continuous magnitude and direction of r, ranging from blue ($r = -1$) through white ($r = 0$) to red ($r = 1$).

3. Results

3.1. CT_{max} during salinity acclimation

During FW acclimation, CT_{max} in SW controls remained stable at 37.6°C (pooled average) throughout the experiment (Fig. 1A). In the FW (salinity transferred) fish, CT_{max} gradually and significantly decreased throughout the experiment, reaching approximately 36°C (Fig. 1A). During SW acclimation, CT_{max} in FW controls remained stable at 34.9°C (pooled average) (Fig. 1B), while in the SW (salinity transferred) fish, CT_{max} gradually and significantly increased throughout the experiment, stabilizing at approximately 36.9°C (Fig. 1B). In both experiments, CT_{max} was significantly affected by salinity, time, and their interaction (two-way ANOVA) and differences in CT_{max} between salinities were detected at every time point after salinity transfer (Sidak's *post hoc* analysis).

3.2. Physiological responses during salinity acclimation and at CT_{max}

In samples taken from fish at T_{acc} during FW acclimation, plasma osmolality and chloride levels did not differ between FW (transferred) and SW (control) groups (Fig. 2A–B). However, plasma cortisol was significantly elevated in FW-transferred fish on day 3 and significantly reduced on day 13 compared to SW controls (Fig. 2C). On day 13, lower gill NKA activity was also observed in SW fish than FW (Fig. 2D). In samples taken from fish at T_{acc} during SW acclimation, no differences in

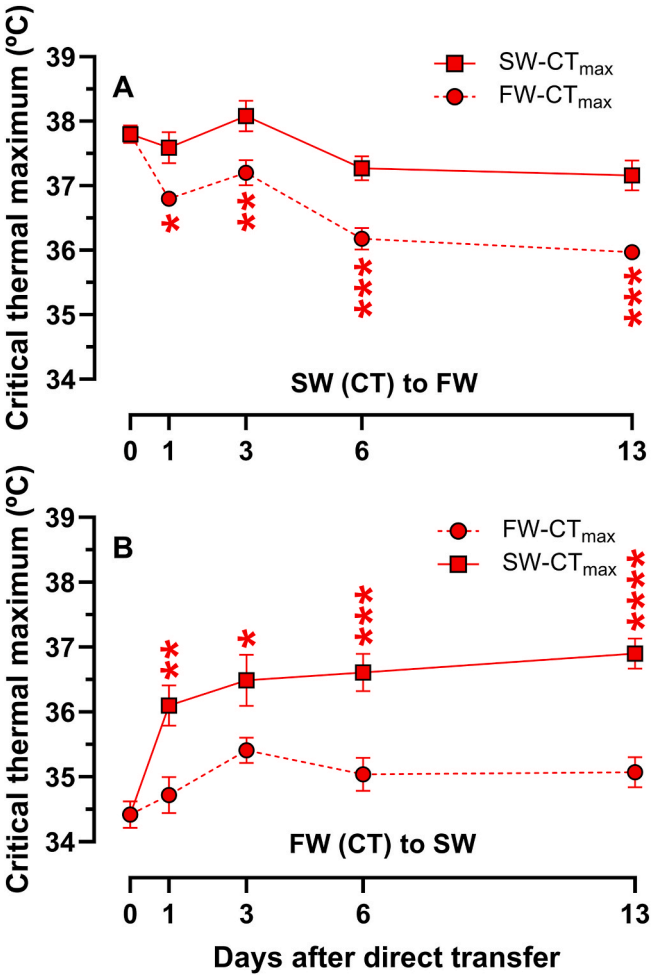


Fig. 1. Critical thermal maximum ($CT_{max;}$ °C) in mummichog during either SW to FW (A) or FW to SW (B) transition at 0, 1, 3, 6, and 13 days post-direct transfer. Data are presented as mean ± SEM (n = 10–11 per salinity and day); *significant difference between salinity at respective time points (two-way ANOVA, Sidak's *post hoc*). *$P \leq 0.05$; **$P \leq 0.01$; ***$P \leq 0.001$; ****$P \leq 0.0001$. Further statistical information is in Supplementary Tables 1 and 2 (three-way ANOVAs).

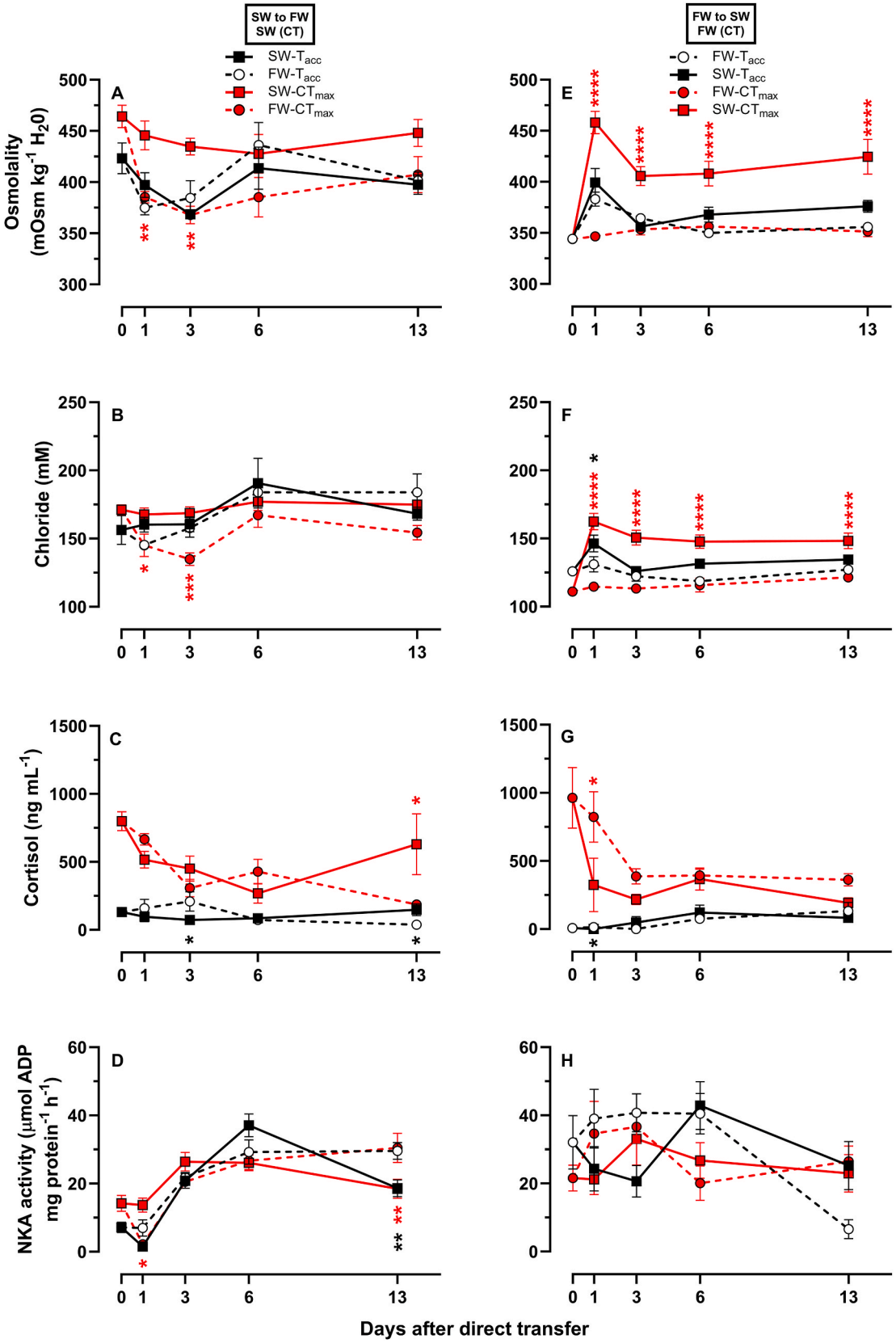


Fig. 2. Osmoregulatory responses in mummichog during either SW to FW (A-D) or FW to SW (E-H) transition at 0, 1, 3, 6, and 13 days post-direct transfer. All values are for plasma, except for NKA activity (from gill). Black asterisks* indicate significant differences between T_{acc} salinities for a given time point. Red asterisks* indicate significant differences between CT_{max} salinities for a given time point. Further details are in legend Fig. 1.

plasma osmolality were detected between SW (transferred) and FW (control) groups (Fig. 2E), although a significant transient increase in plasma chloride in SW (transferred) fish was observed on day 1 (Fig. 2F). Plasma cortisol showed a significant transient decrease in the SW-transferred group relative to FW controls (Fig. 2G), while no differences in gill NKA activity were detected between salinity groups (Fig. 2H).

In samples taken from fish at CT_{max} during salinity acclimation trials, salinity-dependent changes in physiological parameters were much more pronounced. During FW acclimation, FW fish at CT_{max} exhibited reduced plasma osmolality and chloride levels (compared to the SW controls) at days 1 and 3 post-transfer (Fig. 2A–B). However, during SW acclimation, SW fish at CT_{max} exhibited elevated plasma osmolality and chloride (compared to the FW controls) at all days post-transfer (Fig. 2E–F). Generally, regardless of salinity, cortisol was significantly elevated in fish at CT_{max} and not different between salinities (Fig. 2C–G). Exposure to CT_{max} had no observable effect on gill NKA activity (Fig. 2D–H).

In samples taken at T_{acc} during salinity-acclimation trials we observed significant differences in hematocrit, plasma glucose, lactate, or triglycerides levels between salinity-transferred and control fish (Fig. 3A–H). During the SW-to-FW transfer, hematocrit was elevated on day 3, and plasma glucose and lactate were increased on day 1 in FW-transferred fish (Fig. 3A–C). On the other hand, during the FW-to-SW transfer, plasma glucose increased on day 1 (Fig. 3F) and triglycerides increased on day 13 in SW-transferred fish (Fig. 3H). At CT_{max}, hematocrit, plasma glucose, and lactate were significantly elevated in all fish regardless of salinity (Fig. 3A–C, E–G). However, SW-transferred fish exhibited significantly lower plasma triglycerides on day 3 post-transfer compared with FW controls (Fig. 3H).

3.3. Multivariate drivers and physiological correlates of CT_{max}

To elucidate the underlying architecture of thermal tolerance in *Fundulus heteroclitus*, we utilized a multi-stage systems analysis, beginning with model selection via the Second-order Akaike Information Criterion (AICc) to identify the primary environmental and physiological drivers of CT_{max}. This broad-scale modeling approach was subsequently refined through Pearson correlation clusters and multiple targeted regression analyses to pinpoint the specific physiological bottlenecks that could define the upper thermal limit in FW *versus* SW environments.

Model selection via AICc identified the interaction between salinity and acclimation day (Salinity × Day) as the primary driver of thermal tolerance, providing a vastly superior fit (ΔICc = 343.05) and explaining 59.9% of the observed variance in individual thermal tolerance ($R^2 = 0.599$) compared to models relying on body mass alone (Table 1). Initial assessment of fish body mass revealed that size was not uniform across all experimental groups, with a significant interaction detected between salinity and acclimation day (Two-way ANOVA; $F_{3,172} = 18.31$, $p < 0.0001$). This indicated that sampling cohorts were biased by fish size over the course of the experiments. To account for this and isolate the true physiological effect of the treatments, body mass was included as a covariate in a Type III ANCOVA. This analysis confirmed that while mass was a significant covariate ($F_{1,112} = 8.00$, $p = 0.005$), the interaction between salinity and acclimation day remained highly significant ($F_{3,152} = 24.25$, $p < 0.0001$; Table 2). Moreover, ANCOVA confirmed that Salinity × Day model was highly significant ($F_{3,138} = 24.25$, $p = 3.98x10^{-13}$), a result that remained robust after accounting for the significant influence of body mass ($p = 0.005$). The essential role of this interaction was further underscored by a marked increase in AICc (from −75.51 to −17.70) upon its removal from the full model (*i.e.*, Mass + Sal × day). These combined information-theoretic and frequentist analyses demonstrate that the divergent thermal trajectories—a decline in CT_{max} for FW and an increase for SW—are a fundamental physiological response to salinity and not an artifact of cohort size differences.

Systems-level analysis via Pearson correlation matrices and heatmaps (Fig. 4) revealed that the physiological architecture of thermal tolerance diverged significantly between salinity treatments. Note that body mass was excluded from this analysis since sampling cohorts were biased by fish size over the course of the experiment as previously mentioned. In both environments, acclimation time was a primary driver of physiological responses, although its relationship with thermal tolerance differed markedly between salinities. CT_{max} declined strongly with time in FW ($r = -0.73$; Fig. 4A) but increased in SW ($r = 0.54$; Fig. 4B), indicating opposite acclimatory trajectories depending on osmotic environment. A similar reversal was observed for residual ATPase activity (Res), which increased over time in FW (r with day = 0.58; Fig. 4A) but decreased in SW ($r = -0.37$; Fig. 4B), consistent with a higher energetic burden during FW acclimation and a progressive stabilization in SW.

In FW (Fig. 4A), thermal tolerance appeared primarily constrained by ionic regulation and energetic costs. Plasma chloride declined moderately with acclimation time ($r = -0.38$), while Res increased strongly, suggesting that maintaining ion balance in low salinity imposed increasing metabolic demand. Accordingly, CT_{max} was positively associated with plasma chloride (Cl; $r = 0.42$) and negatively associated with Res ($r = -0.41$). In contrast, these ionic relationships weakened in SW (Fig. 4B), where CT_{max} showed only a weak association with chloride ($r = 0.19$). Instead, thermal performance in SW was more closely linked to metabolic and osmotic state, with CT_{max} positively correlated with lactate (Lact; $r = 0.62$), glucose (Gluc; $r = 0.31$), cortisol (F; $r = 0.32$), and osmolality (Osm; $r = 0.23$).

Several relationships were conserved across salinities. Lactate was positively correlated with CT_{max} in both FW ($r = 0.43$; Fig. 4A) and SW ($r = 0.62$; Fig. 4B), suggesting that anaerobic metabolic capacity contributes to thermal tolerance regardless of osmotic environment. Similarly, the relationships between triglycerides and Res, as well as chloride and Res, were maintained across both treatments. However, other associations were salinity specific. In FW, cortisol and hematocrit covaried strongly ($r = 0.50$; Fig. 4A). FW fish also exhibited multiple significant day-dependent relationships involving chloride, lactate, NKA, and triglycerides. By contrast, SW fish showed stronger integration between CT_{max} and osmotic/metabolic indicators.

To reduce collinearity in subsequent multiple linear regressions and retain independent mechanistic predictors, several highly redundant variable pairs were excluded. Osmolality and chloride were strongly correlated, particularly in SW ($r = 0.73$; FW = 0.56). Likewise, NKA and residual ATPase activity showed strong redundancy in both groups (SW = 0.78; FW = 0.72). Lactate and glucose were also moderately but consistently correlated in both salinities ($r \approx 0.54$), supporting the use of lactate as the principal proxy for anaerobic metabolic scope. The final analysis therefore focused on four non-collinear axes associated with thermal tolerance: acclimation time/salinity, ionic stability (Cl), metabolic state (Lac), and energetic overhead (Res).

4. Discussion

The present study aimed to provide insights into the interaction of environmental temperature and salinity on the physiology of mummichog (*F. heteroclitus*), an eurythermal and euryhaline model fish species, throughout convergent statistical approaches. Both univariate analyses (Two-way ANOVA) and multivariate modeling (AICc-based selection and Type III ANCOVA) consistently demonstrated that the interaction between salinity and acclimation duration is the primary determinant of thermal tolerance. Our findings demonstrate that fish acclimated to SW exhibited up to 2.7°C higher (pooled averages) CT_{max} compared to those acclimated to FW. Earhart et al. (2024) found no CT_{max} difference between 3 and 20 ppt, our use of 38 ppt aligns with their reported CT_{max} of ~37.5°C, supporting the hypothesis that the observed divergence is driven by the physiological costs of ion-poor environments (FW) reducing thermal limits rather than SW increasing them above a typical

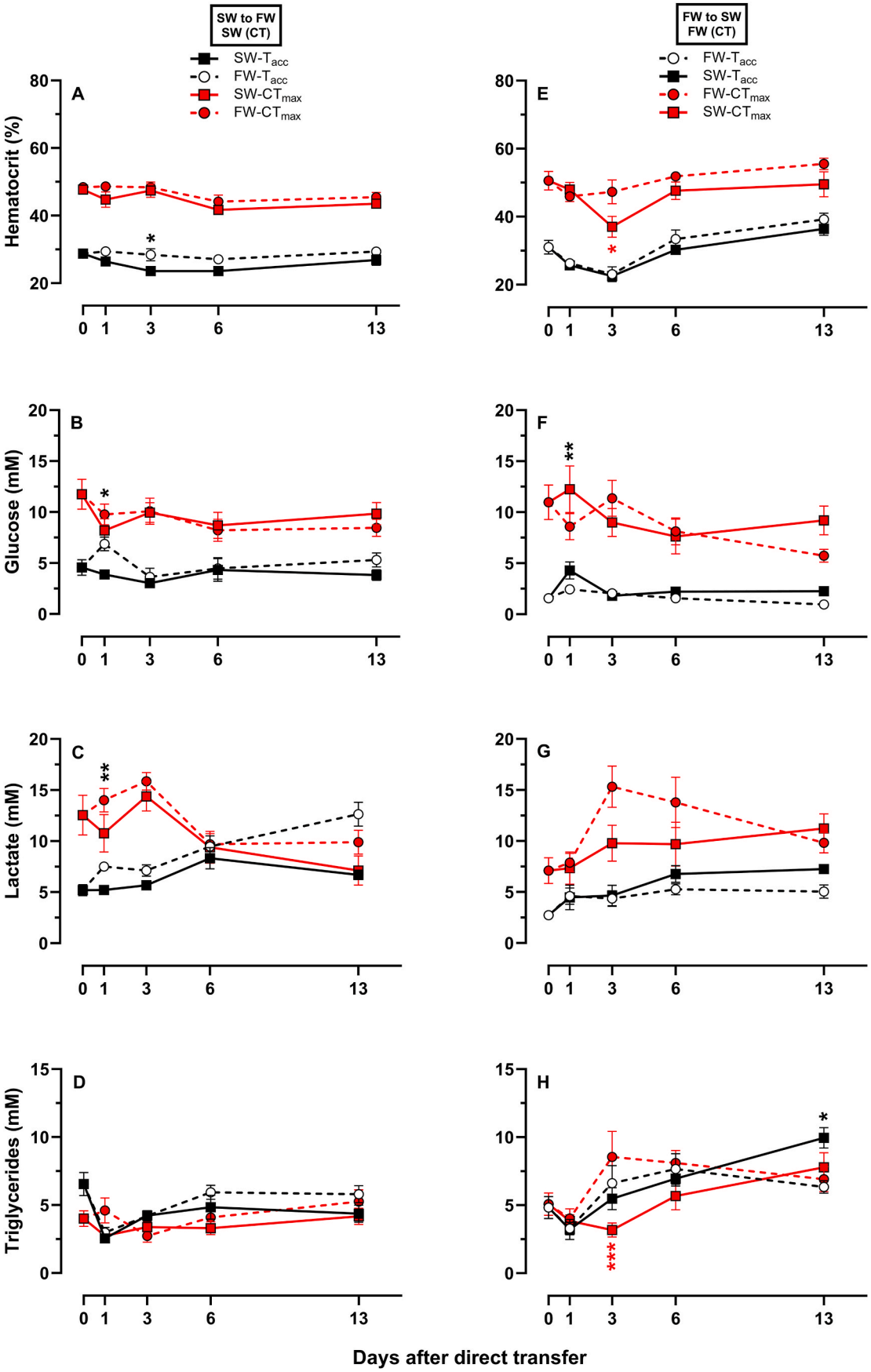

SW to FW
SW (CT)
SW-T$_{acc}$
FW-T$_{acc}$
SW-CT$_{max}$
FW-CT$_{max}$
FW to SW
FW (CT)
FW-T$_{acc}$
SW-T$_{acc}$
FW-CT$_{max}$
SW-CT$_{max}$
A
B
C
D
E
F
G
H
Hematocrit (%)
Glucose (mM)
Lactate (mM)
Triglycerides (mM)
Days after direct transfer
0 1 3 6 13

Fig. 3. Metabolic-stress responses in mummichog during either SW to FW (A-D) or FW to SW (E-H) transitions and after exposure to critical thermal maximum testing (CT_{max}) at 0, 1, 3, 6, and 13 days post-direct transfer. All values are for plasma, except for hematocrit (whole blood). Further details are in legends of Figs. 1 and 2.

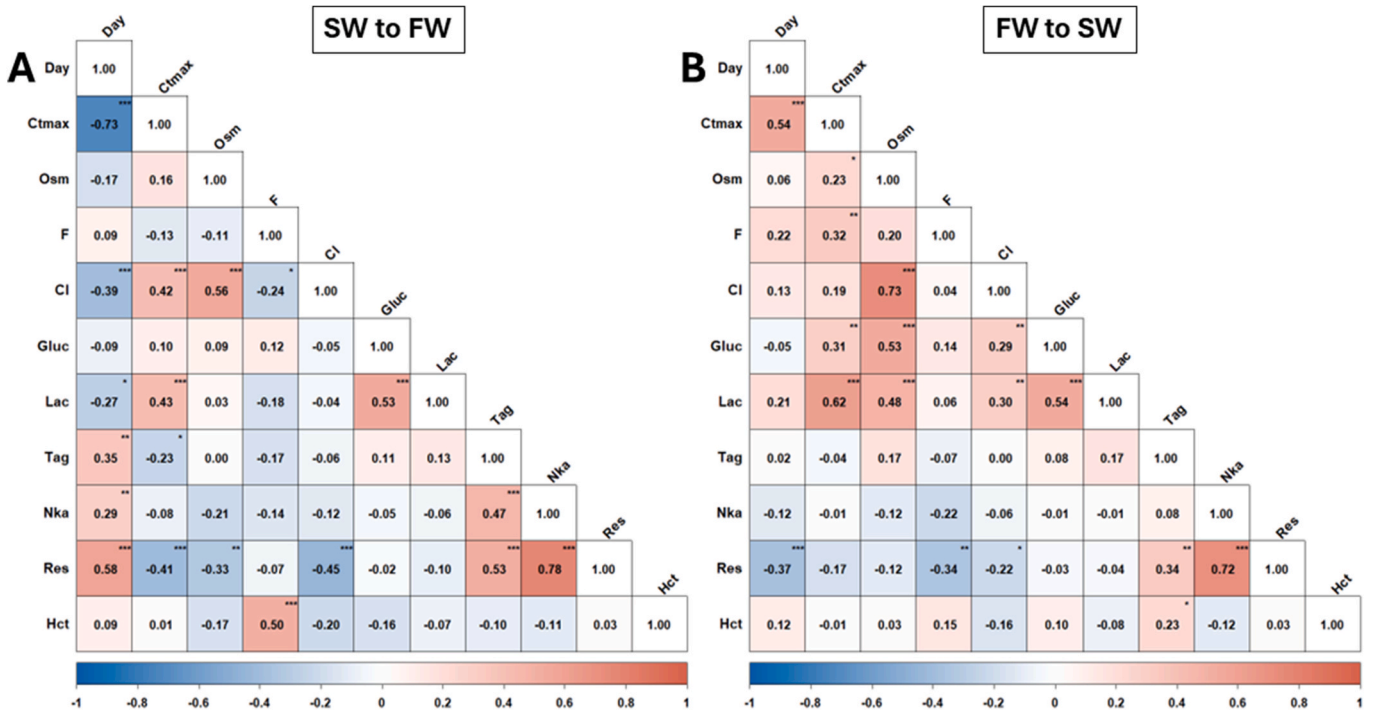


Fig. 4. Correlation matrix of candidate physiological drivers of thermal tolerance in either SW to FW (A) or FW to SW (B) transitions and after exposure to critical thermal maximum testing (CT_{max}). In this system-level analysis, fish acclimated to their original salinity for ≥4 weeks were integrated into the Day 13 cohort to represent the stable physiological plateau reached at the conclusion of the acclimation trajectory (*AIC.CTmax* file provided in the supplementary files). Colors and values represent Pearson's coefficients (r). Abbreviations: CTmax: Critical thermal tolerance; Sal: Salinity; Cl: chloride; Lac: lactate; Res: residual-ATPase ouabain insensitive; Day: experimental day; F: cortisol; Osm: osmolality; Glc: glucose; Tag: triglycerides; Nka: Na^+/K^+-ATPase; Hct: hematocrit. Cell color represented the magnitude and direction of correlations, ranging from blue (r = −1) through white (r = 0) to red (r = 1). Significance levels were indicated with asterisks (*$P < 0.05$, **$P < 0.01$, ***$P < 0.001$).

baseline.

Initial exploration identified body mass as a significant covariate, subsequent ANCOVA and AICc selection confirmed that the Salinity × Day interaction remained the overwhelming dominant predictor (ΔICc of 343.05; ΔICcWt = 99.99%) that explained ~60% of the observed variability in CT_{max} (R^2 = 0.599). This ensures that the divergent thermal trajectories—a decline in CT_{max} for FW and an increase for SW—represent a fundamental physiological response to osmotic challenge rather than an artifact of cohort size differences. Although our study fails on addressing influence of Size-Dependent Thermal Tolerance (SDTT), the relationship between fish size and CT_{max} remains unresolved in fishes, with studies reporting positive, neutral, or negative associations depending on species and experimental context (Gomez Isaza and Rodgers, 2024). Body size may nevertheless influence other physiological boundaries relevant to thermal performance. Larger individuals often exhibit greater osmoregulatory capacity during salinity transitions, whereas smaller fish may respond more rapidly to acute osmotic stress (Parry, 1958; McCormick and Naiman, 1984; Bjerknes et al., 1992; Allen et al., 2011; Styga et al., 2019). Similarly, larger-bodied fish can become more vulnerable under combined warming and hypoxic conditions due to higher metabolic demand (Verberk et al., 2022; Deutsch et al., 2022; Hvas et al., 2025). These interactions suggest that body size may indirectly influence thermal tolerance through its effects on ionoregulatory and metabolic performance, highlighting the need for further investigation of size-dependent responses across fluctuating osmotic environments and different taxa.

The contrasting CT_{max} responses between salinities were accompanied by distinct physiological constraints. By removing redundant variables, our system-level analysis using Pearson correlation matrices for each salinity identified four non-collinear correlates of thermal tolerance: the salinity–acclimation time axis, ionic stability (plasma chloride, Cl^-), metabolic state (plasma lactate, Lac), and energetic overhead (ouabain-insensitive residual gill ATPase activity, Res). In FW, thermal tolerance was primarily associated with the interaction between ionic stability and energetic demand, reflected by the stronger inverse relationship between Cl and Res (r = −0.45; Fig. 4A). This pattern suggests that maintaining ion balance in low salinity imposes a substantial energetic cost that reduces thermal tolerance. In contrast, this relationship weakened in SW, where CT_{max} was more strongly associated with metabolic indicators, particularly lactate (r = 0.62; Fig. 4B). Together, these results indicate that FW fish may reach thermal limits under increasing ionoregulatory stress, whereas SW fish maintain greater ionic stability and are instead constrained by metabolic and anaerobic capacity at high temperatures.

Previous studies in the stenohaline marine fish Gilthead seabream (*Sparus auratus*), 35-day acclimation to different salinities and temperatures showed that the interaction between salinity and temperature elicits distinct physiological responses: gill Na^+/K^+-ATPase is upregulated under hyperosmotic and elevated thermal conditions to preserve ionic homeostasis, whereas renal Na^+/K^+-ATPase capacity remains salinity-invariant but increases with temperature; concomitantly, hepatic metabolic pathways are reorganized in response to combined salinity–temperature stress. Extreme salinity exposure induces cortisol elevations indicative of chronic stress, yet lower temperatures attenuate

the energetic costs of osmoregulation, highlighting that osmoregulatory energy demand is modulated by thermal context (Vargas-Chacoff et al., 2009, 2020). In our study, fish sampled at T_{acc}, levels of gill NKA activity were generally high in both FW and SW and did not show a salinity-dependent response in either salinity transfer experiment. Our observations of only minor changes in physiological indicators of osmoregulatory or general stress during salinity acclimation are consistent with the reported highly euryhaline nature of mummichog (Wood and Marshall, 1994). This reflects previous findings of a relatively small influence of salinity on gill NKA activity in mummichog, which may relate to their preferred intertidal marsh which has large tidal-driven fluctuations in salinity (Marshall et al., 1999) although the existence of rapid changes in gill NKA activity, not detected in the study due to not using proper timing, cannot be ruled out (Mancera and McCormick, 2000).

While the initial decline in CT_{max} within FW-acclimated cohorts aligns with a critical window of acute ionoregulatory vulnerability (days 1–3; Fig. 2A and B), the failure of thermal tolerance to recover by day 13—despite the restoration of apparent ionic stability—suggests a fundamental shift in the fish's physiological steady-state. Our multivariate analysis provides a likely explanation of this permanent thermal penalty: as plasma chloride levels stabilize in FW (from day 6 onwards; Fig. 2A and B), mummichogs transition toward a heavy reliance on ouabain-insensitive insensitive or residual ATPase activity occurred ($r = 0.58$ with acclimation time; Fig. 4A). This upregulation is a recognized compensatory strategy for active ion uptake in ion-poor environments, where fish often shift their enzymatic reliance from ouabain-sensitive Na^+/K^+-ATPase to alternative ATPase to maintain homeostasis against steep osmotic gradients (Pfeiler and Kirschner, 1972; Ventrella et al., 1992; Mayer-Gostan and Naon, 1992; Evans et al., 2005). Additionally, FW fish exhibited multiple significant day-dependent relationships involving chloride, lactate, NKA, and triglycerides, indicating a broader, highly dynamic physiological reorganization through time.

As suggested by Monette et al. (2025), warm-temperature acclimation can impair hyper-osmoregulatory performance in killifish—specifically freshwater (FW) ionoregulation—by down-regulating *ncc2*, the primary passive transporter for FW NaCl uptake. Reduced NCC2 capacity at elevated temperatures likely weakens active ion uptake, forcing fish to rely on auxiliary, metabolically costly pathways to counter passive ion loss. In our study, during the SW-to-FW transition, the inverse relationship between chloride and residual ATPase activity was stronger ($r = -0.45$; Fig. 4A) than during FW-to-SW acclimation ($r = -0.22$; Fig. 4B), indicating that FW ionoregulatory maintenance imposes a more direct energetic constraint. The weaker association in SW suggests greater metabolic flexibility under hyperosmotic conditions. In contrast, SW-acclimated fish showed stronger integration between CT_{max} and osmotic/metabolic indicators (plasma osmolality, glucose, cortisol), consistent with a more stable ionic environment in which ionic markers become largely decoupled from upper thermal limits ($r = 0.19$ for Cl–CT_{max}). Conversely, FW-acclimated fish experience a sustained energetic overhead (Res–CT_{max}; $r = -0.41$) that directly depresses thermal performance. This hypoosmotic challenge is further reflected in a strong cortisol–hematocrit covariation ($r = 0.50$; Fig. 4A), suggesting a stress-linked erythropoietic response unique to FW acclimation. Together, these patterns indicate that chronic hyper-osmoregulatory costs limit thermal performance, producing a lower thermal plateau and preventing CT_{max} recovery even after apparent osmotic balance is restored. This aligns with observations in other euryhaline species, which exhibit narrower thermal ranges in non-natal osmotic regimes. Overall, warm temperatures reduce the efficiency of FW ionoregulatory mechanisms, and the combined demands of ionoregulation and heat impose a sustained energetic burden, particularly for non-FW-native species (Nakamura et al., 2020).

During the FW-to-SW transfer, plasma osmolality and chloride increased significantly at CT_{max} by day 1 and remained elevated through day 13 (Fig. 2E and F). This persistent elevation, occurring alongside a progressive rise in CT_{max} ($r = 0.54$; Fig. 4B), indicates that long-term SW-acclimated mummichogs cope more effectively with concurrent thermal and osmotic stress than recently transferred fish. Our Pearson correlation analysis shows that this thermal improvement is supported by a distinct physiological architecture in which ionic markers decouple from upper thermal limits ($r = 0.19$ for Cl–CT_{max}). Instead of being constrained by ionoregulatory demands, thermal performance in SW becomes more tightly linked to metabolic and stress indicators, showing positive correlations with lactate ($r = 0.62$), glucose ($r = 0.31$), and cortisol ($r = 0.32$). This transition is accompanied by a decline in metabolic overhead, reflected in decreasing residual ATPase activity ($r = -0.37$ with day; Fig. 4B) and a weaker Cl–Res association ($r = -0.22$). This coordinated response suggests enhanced metabolic flexibility under hyperosmotic conditions, enabling SW fish to stabilize physiologically and progressively expand their thermal tolerance.

While previous literature often emphasizes cellular stress proteins such as heat shock proteins (Dubeau et al., 1998;Todgham et al., 2005; Metzger et al., 2016), our data suggests that at the whole-organism level, the individual's ability to manage this metabolic load and maintain osmotic integrity may define the functional limits. Although this could suggest heightened vulnerability of intertidal mummichogs to thermal stress, natural daily salinity fluctuations may also train these fish through repeated mild osmotic challenges, enhancing their osmoregulatory flexibility (Moorman et al., 2015)—a phenomenon similarly observed in thermally fluctuating environments compared with constant laboratory temperatures (Monette et al., 2025). Our direct-transfer protocol—abruptly shifting fish between FW and SW without gradual salinity adjustment—fails to mimic this conditioning and may therefore overestimate thermal susceptibility in wild populations. Such acquired resilience reflects physiological plasticity, whereby prior exposure to variable salinities enhances tolerance to subsequent stressors, suggesting that naturally "intertidal-trained" mummichogs may better withstand abrupt environmental changes than our protocol implies (Schreck and Tort, 2016). Overall, the influence of salinity transfer on physiological indicators of metabolic stress was minor compared to the robust response of these physiological parameters to elevated temperature. The massive increases in plasma cortisol, glucose, and lactate following exposure to elevated temperature are consistent with an activation of the primary and secondary stress responses, which have been observed in several fish species (Wendelaar Bonga, 1997; Mommsen et al., 1999; Ern et al., 2023). However, our findings suggest that while the endocrine response is universal, the ultimate bottleneck defining the thermal limit is environment-specific, shifting from ionic stability in FW to metabolic scope in SW. Nevertheless, it is important to acknowledge that some of the physiological changes observed at CT_{max} may not be causal determinants of thermal tolerance but rather consequences of the CT_{max} test itself. Because individuals with higher CT_{max} experience higher temperatures for longer durations, elevated lactate, glucose, or cortisol may partly reflect the acute metabolic and endocrine demands of the heating protocol rather than pre-existing differences that set the thermal limit. This possibility does not negate the environment-specific patterns we report, but it highlights the need for caution when interpreting end-point physiological measurements as mechanistic drivers of CT_{max} rather than as integrated responses to extreme thermal exposure.

Fry and Hart (1948) initially described the relationship between aerobic scope and temperature, observing that standard metabolic rate increases with temperature until maximum oxygen uptake plateaus or declines. This formed the basis for the oxygen- and capacity-limited thermal tolerance (OCLTT) hypothesis, which suggests that CT_{max} is determined by the cardiorespiratory system's inability to meet tissue O_2 demand at elevated temperatures (Pörtner, 2014; Pörtner et al., 2017). In mummichog, the reduction in thermal tolerance following FW exposure likely stems from impaired branchial oxygen uptake or delivery. Specifically, FW acclimation in this species reduces hypoxia tolerance, a shift associated with structural gill remodeling: reduced

lamellar surface area, thickened epithelia, and increased interlamellar cell mass (ILCM), all of which increase water–blood diffusion distance (Giacomin et al., 2019). Crucially, these tissue-level morphological changes (i.e., ILCM) should be distinguished from the functional cellular remodeling of the gill epithelium. While FW acclimation involves a transformation from a salt-secreting surface in SW to a salt-absorbing surface in FW—requiring extensive remodeling of ionocytes and ion-transport pathways (Zimmer and Perry, 2022; Inokuchi et al., 2022)—it is currently unclear if ionocyte proliferation directly contributes to the development of ILCM. In mummichog, Giacomin et al. (2019) did not provide evidence that ionocytes were the specific cell types responsible for these morphological differences. Therefore, any causal link between ionocyte remodeling and physical lamellar obstruction remains hypothetical.

Freshwater teleosts rely on the active uptake of Na^+ and Cl^- by gill is critical to the survival of all fish in FW, carried out by specialized ionocytes on the gill surface, which are upregulated under ion-poor or low-Na^+/Cl^- conditions (Evans et al., 2005; Dymowska et al., 2012). Interestingly, and unlike many other teleosts, *Fundulus heteroclit*us, *Anguilla spp.,* and *Lepomis macrochirus* do not actively uptake Cl^- at the gills in FW—a trait attributed to the absence of typical FW chloride cells (Hyde and Perry, 1987; Laurent et al., 2006; Evans, 2011)—yet these species can tolerate rapid osmotic transitions. At the molecular level, mummichog expresses *ncc2* mRNA in a pattern consistent with the classic FW ion-uptake model, but under a scenario where branchial Cl^- uptake is not observed the ultimate fate of Cl^- that would be cotransported with Na^+ by NCC2 remains unclear (Breves et al., 2020). Concurrent expression of *nkcc1* and *cftr* further indicates that SW-type ionocytes are maintained in a "ready state" even when mummichogs inhabit FW (Karnaky, 1986; Breves et al., 2020). This maintenance of SW-type ionocytes may provide a mechanistic basis for why CT_{max} measured in SW appears largely independent of the duration of FW acclimation: the ionocyte complement required for SW function is already present and can be rapidly mobilized upon transfer to SW. In contrast, the overall respiratory capacity in FW may be hindered by the aforementioned morphological changes (e.g., ILCM and thickened epithelium). This represents a classic osmorespiratory compromise as previously explained. The structural barriers (ILCM and thickened epithelia) formed to minimize diffusive ion loss in FW simultaneously restrict oxygen uptake during the high-demand conditions of a thermal ramp. This physical restructuring, combined with the metabolic costs of ionocyte activation, may impair oxygen delivery—via altered cardiac performance or reduced peripheral O_2 off-loading—thereby lowering thermal tolerance (Wood et al., 2019; Morgenroth et al., 2019, 2022; Ruhr et al., 2020). Further work should examine how FW exposure alters gill oxygen uptake, cardiac function, and tissue oxygenation in mummichog, and should also investigate alternative mechanisms of Cl^- uptake, particularly given the unexpected increase in plasma Cl^- from day 6 onwards in FW acclimated fish following CT_{max} trial (Fig. 2B). Such studies would help clarify whether mummichog employ non-classical or compensatory Cl^- transport pathways under FW and heat stress conditions.

4.1. Conclusion

While euryhaline species comprise only 4% of known fishes, they are ecological keys in the world's most dynamic aquatic environments (i.e., estuaries, coastal lagoons, mangrove habitats and tidal marshes). Our findings demonstrate that for one of these model species (*F. Heteroclitus*), critical thermal maximum (CT_{max}) is not a fixed physiological trait, but a dynamic state governed by the interaction of salinity and acclimation time. Specifically, in the mummichog, the transition to FW imposes a thermal tax that significantly reduces heat tolerance immediately. Recent global analyses suggest that FW-specialist fishes exhibit greater thermal tolerance and plasticity than marine species (Verberk et al., 2026); however, our study highlights a key limitation of such generalizations for euryhaline models. Although these fish occupy thermally variable environments, their capacity to acclimate to elevated temperatures is strongly modulated by osmotic context with mummichog at low salinities (0–3 ppt) failing to achieve the higher thermal tolerance observed under SW conditions. Together, these findings emphasize the need to prioritize habitat-specific stressors over broad latitudinal patterns when predicting climate vulnerability, linking thermal limits directly to environmentally fluctuating salinities. Consequently, current ecological forecasts likely underestimate risk to these types of fish populations, since low salinity may create a lethal physiological bottleneck. Incorporating salinity as a primary co-stressor in ecological models is therefore essential; only by moving beyond single-stressor paradigms can we accurately assess the resilience of estuarine ecosystems in an increasingly warm and salinity-variable scenario.

Ethics statement

This research conformed to the University of Cadiz (UCA) animal protection guidelines, Spanish Royal Decree 53/2013, and EU Directive 86/609/EU under permit No. 28-04-15-241 from the Junta de Andalucía Ethics and Animal Welfare Committee.

Funding

This research did not receive any specific grant from funding agencies in the public, commercial, or not-for-profit sectors. A.B. was supported by a Margarita Salas Postdoctoral Research Fellowship at the University of Massachusetts Amherst, funded by the University of Cádiz (Spain) and the European Union through the NextGenerationEU recovery instrument. A.C. is supported by a Ph.D. fellowship from the Regional Government of Andalusia, Spain (Reference: PREDOC_02015). P.S.M. was supported by a Juan de la Cierva-Formación Postdoctoral Research Fellowship (Reference: FJCI-2021-047759-I) funded by the Spanish Ministry of Science and Innovation.

CRediT authorship contribution statement

André Barany: Data curation, Formal analysis, Investigation, Methodology, Software, Visualization, Writing – original draft, Writing – review & editing. **Anyell Caderno:** Data curation, Formal analysis, Methodology, Software, Visualization, Writing – review & editing. **Paula Simó-Mirabet:** Data curation, Formal analysis, Methodology, Writing – review & editing. **Ciarán Alvar Shaughnessy:** Data curation, Formal analysis, Investigation, Methodology, Software, Visualization, Writing – review & editing. **Juan Antonio Martos-Sitcha:** Conceptualization, Resources, Supervision, Writing – review & editing. **Juan Miguel Mancera:** Conceptualization, Funding acquisition, Project administration, Resources, Writing – review & editing. **Stephen Daniel McCormick:** Conceptualization, Investigation, Methodology, Supervision, Writing – review & editing.

Declaration of competing interest

The authors declare that they have no known competing financial interests or personal relationships that could have appeared to influence the work reported in this paper.

Acknowledgments

We thank Sara del Carmen Flores Moreno, Rubén Galindo Melero, and Paloma Fernández Morell for their help and assistance during the samplings.

Appendix A. Supplementary data

Supplementary data to this article can be found online at https://doi.org/10.1016/j.jtherbio.2026.104531.

Data availability

All relevant data supporting this study are provided as Supplementary Material.

References

Allen, P.J., McEnroe, M., Forostyan, T., et al., 2011. Ontogeny of salinity tolerance and evidence for seawater-entry preparation in juvenile green sturgeon. Acipenser. Medirostr. J. Compar. Physiol. B 181, 1045–1062. https://doi.org/10.1007/s00360-011-0592-0.

Andreassen, A.H., Hall, P., Khatibzadeh, P., Jutfelt, F., Kermen, F., 2022. Brain dysfunction during warming is linked to oxygen limitation in larval zebrafish. Proc. Natl. Acad. Sci. 119 (39), e2207052119. https://doi.org/10.1073/pnas.2207052119.

Barrionuevo, W.R., Femandes, M.N., 1995. Critical thermal maxima and minima for curimbatá, *Prochilodus scrofa* Steindachner, of two different sizes. Aquac. Res. 26 (6), 447–450. https://doi.org/10.1111/j.1365-2109.1995.tb00934.x.

Becker, C.D., Genoway, R.G., 1979. Evaluation of the critical thermal maximum for determining thermal tolerance of freshwater fish. Environ. Biol. Fish. 4 (3), 245–256. https://doi.org/10.1007/BF00005481.

Bernardi, G., Fernandez-Delgado, C., Gomez-Chiarri, M., Powers, D.A., 1995. Origin of a Spanish population of *Fundulus heteroclitus* inferred by cytochrome b sequence analysis. J. Fish. Biol. 47 (4), 737–740. https://doi.org/10.1111/j.1095-8649.1995.tb01939.x.

Bjerknes, V., Duston, J., Knox, D., Harmon, P., 1992. Importance of body size for acclimation of underyearling Atlantic salmon parr (*Salmo salar* L.) to seawater. Aquaculture 104 (3–4), 357–366. https://doi.org/10.1016/0044-8486(92)90216-8.

Breves, J.P., Starling, J.A., Popovski, C.M., et al., 2020. Salinity-dependent expression of ncc2 in opercular epithelium and gill of mummichog (*Fundulus heteroclitus*). J. Comp. Physiol. B 190, 219–230. https://doi.org/10.1007/s00360-020-01260-x.

Bulger, A.J., Tremaine, S.C., 1985. Magnitude of seasonal effects on heat tolerance in *Fundulus heteroclitus*. Physiol. Zool. 58 (2), 197–204. http://www.jstor.org/stable/30158567.

Burnham, K.P., Anderson, D.R., 2002. Model Selection and Inference: a Practical Information-Theoretic Approach, second ed. Springer-Verlag, New York. https://doi.org/10.1007/b97636.

Chen, J.-C., Chen, W.-C., 1999. Temperature tolerance of *Haliotis diversicolor* at different salinity and temperature levels. Comp. Biochem. Physiol. Mol. Integr. Physiol. 124 (1), 73–80. https://doi.org/10.1016/s1095-6433(99)00092-6.

Cheng, S.-Y., Chen, C.-S., Chen, J.-C., 2013. Salinity and temperature tolerance of brown-marbled grouper *Epinephelus fuscoguttatus*. Fish Physiol. Biochem. 39 (2), 277–286. https://doi.org/10.1007/s10695-012-9698-x.

Christensen, E.A.F., Norin, T., Tabak, I., van Deurs, M., Behrens, J.W., 2021. Effects of temperature on physiological performance and behavioral thermoregulation in an invasive fish, the round goby. J. Exp. Biol. 224 (1). https://doi.org/10.1242/jeb.237669.

Comte, L., Olden, J.D., 2017. Evolutionary and environmental determinants of freshwater fish thermal tolerance and plasticity. Glob. Change Biol. 23 (2), 728–736. https://doi.org/10.1111/gcb.13427.

Currie, R.J., Bennett, W.A., Beitinger, T.L., 1998. Critical thermal minima and maxima of three freshwater game-fish species acclimated to constant temperatures. Environ. Biol. Fish. 51 (2), 187–200. https://doi.org/10.1023/A:1007447417546.

Dahlke, F.T., Wohlrab, S., Butzin, M., Pörtner, H.-O., 2020. Thermal bottlenecks in the life cycle define climate vulnerability of fish. Science 369 (6499), 65–70. https://doi.org/10.1126/science.aaz3658.

Denisse Re, A., Díaz, F., Ponce-Rivas, E., Giffard, I., Muñoz-Marquez, M.E., Sigala-Andrade, H.M., 2012. Combined effect of temperature and salinity on the Thermotolerance and osmotic pressure of juvenile white shrimp *Litopenaeus vannamei* (Boone). J. Therm. Biol. 37 (6), 413–418. https://doi.org/10.1016/J.JTHERBIO.2012.04.004.

Denisse Re, A., Díaz, F., Valdez, G., 2006. Effect of salinity on the thermoregulatory behavior of juvenile blue shrimp *Litopenaeus stylirostris* stimpson. J. Therm. Biol. 31 (6), 506–513. https://doi.org/10.1016/J.JTHERBIO.2006.05.004.

Deutsch, C., Penn, J.L., Verberk, W.C.E.P., Inomura, K., Endress, M., Payne, J.L., 2022. Impact of warming on aquatic body sizes explained by metabolic scaling from microbes to macrofauna. Proc. Natl. Acad. Sci. 119 (28), e2201345119. https://doi.org/10.1073/pnas.2201345119.

Dubeau, S.F., Pan, F., Tremblay, G.C., Bradley, T.M., 1998. Thermal shock of salmon in vivo induces the heat shock protein hsp 70 and confers protection against osmotic shock. Aquaculture 168 (1–4), 311–323. https://doi.org/10.1016/S0044-8486(98)00358-5.

Dymowska, A.K., Hwang, P.P., Goss, G.G., 2012. Structure and function of ionocytes in the freshwater fish gill. Respir. Physiol. Neurobiol. 184, 282–292.

Earhart, M.L., Thapar, M., Blanchard, T.S., Bugg, W.S., Schulte, P.M., 2024. Persistent interactive effects of developmental salinity and temperature in Atlantic killifish (*Fundulus heteroclitus*). Comp. Biochem. Physiol. Mol. Integr. Physiol. 297, 111732. https://doi.org/10.1016/J.CBPA.2024.111732.

Elliott, J.M., Elliott, J.A., 1995. The effect of the rate of temperature increase on the critical thermal maximum for parr of Atlantic salmon and brown trout. J. Fish. Biol. 47 (5), 917–919. https://doi.org/10.1111/j.1095-8649.1995.tb06014.x.

Ern, R., Andreassen, A.H., Jutfelt, F., 2023. Physiological mechanisms of acute upper thermal tolerance in fish. Physiology 38 (3), 141–158. https://doi.org/10.1152/physiol.00027.2022.

Evans, D.H., 2011. Freshwater fish gill ion transport: august krogh to morpholinos and microprobes. Acta Physiol. 202, 349–359.

Evans, D.H., Piermarini, P.M., Choe, K.P., 2005. The multifunctional fish gill: dominant site of gas exchange, osmoregulation, acid-base regulation, and excretion of nitrogenous waste. Physiol. Rev. 85 (1), 97–177. https://doi.org/10.1152/physrev.00050.2003.

Evans, T.G., Kültz, D., 2020. The cellular stress response in fish exposed to salinity fluctuations. J. Exp. Zool. Part A: Ecological and Integrative Physiology 333 (6), 421–435. https://doi.org/10.1002/jez.2350.

Fangue, N.A., Hofmeister, M., Schulte, P.M., 2006. Intraspecific variation in thermal tolerance and heat shock protein gene expression in common killifish, *Fundulus heteroclitus*. J. Exp. Biol. 209 (15), 2859–2872. https://doi.org/10.1242/jeb.02260.

Feist, S.E., Hoque, M.A., Islam, M.A., Dewan, A., Fowler, M., 2025. Sea-level rise drives changes in salinisation patterns in low-lying Bangladesh. Ecol. Indic. 176, 113543. https://doi.org/10.1016/J.ECOLIND.2025.113543.

Fry, F.E.J., Hart, J.S., 1948. The relation of temperature to oxygen consumption in the goldfish. Biol. Bull. 94 (1), 66–77. https://doi.org/10.2307/1538211.

Garcia-Soto, C., Cheng, L., Caesar, L., Schmidtko, S., Jewett, E.B., Cheripka, A., Rigor, I., Caballero, A., Chiba, S., Báez, J.C., Zielinski, T., Abraham, J.P., 2021. An overview of ocean climate change indicators: sea surface temperature, ocean heat content, ocean pH, dissolved oxygen concentration, arctic sea ice extent, thickness and volume, sea level and strength of the AMOC (Atlantic meridional overturning circulation). Front. Mar. Sci. 8. https://doi.org/10.3389/fmars.2021.642372, 2021.

Giacomin, M., Bryant, H.J., Val, A.L., Schulte, P.M., Wood, C.M., 2019. The osmorespiratory compromise: physiological responses and tolerance to hypoxia are affected by salinity acclimation in the euryhaline Atlantic killifish (*Fundulus heteroclitus*). J. Exp. Biol. 222 (19). https://doi.org/10.1242/jeb.206599.

Gomez Isaza, D.F., Rodgers, E.M., 2024. Upper thermal limits are 'hard-wired' across body mass but not populations of an estuarine fish. J. Therm. Biol. 125, 103970. https://doi.org/10.1016/J.JTHERBIO.2024.103970.

Hall-Scharf, B.J., et al., 2025. How body size and salinity affects thermal tolerance of a range-expanding fish. Marin. Coast. Fish. 17.

Haney, D.C., Walsh, S.J., 2003. Influence of salinity and temperature on the physiology of Limia melanonotata (Cyprinodontiformes: poeciliidae): a search for abiotic factors limiting Insular distribution in Hispaniola. Caribb. J. Sci. 39 (3), 327–337. https://pubs.usgs.gov/publication/70024663.

Healy, T.M., Schulte, P.M., 2012a. Factors affecting plasticity in whole-organism thermal tolerance in common killifish (*Fundulus heteroclitus*). J. Comp. Physiol. B 182 (1), 49–62. https://doi.org/10.1007/s00360-011-0595-x.

Healy, T.M., Schulte, P.M., 2012b. Thermal acclimation is not necessary to maintain a wide thermal breadth of aerobic scope in the common killifish (*Fundulus heteroclitus*). Physiol. Biochem. Zool. 85 (2), 107–119. https://doi.org/10.1086/664584.

Hieu, D.Q., Hang, B.T.B., Huong, D.T.T., Kertaoui, N. El, Farnir, F., Phuong, N.T., Kestemont, P., 2021. Salinity affects growth performance, physiology, immune responses and temperature resistance in striped catfish (*Pangasianodon hypophthalmus*) during its early life stages. Fish Physiol. Biochem. 47 (6), 1995–2013. https://doi.org/10.1007/s10695-021-01021-9.

Hines, C.W., Fang, Y., Chan, V.K.S., Stiller, K.T., Brauner, C.J., Richards, J.G., 2019. The effect of salinity and photoperiod on thermal tolerance of Atlantic and coho salmon reared from smolt to adult in recirculating aquaculture systems. Comp. Biochem. Physiol. Mol. Integr. Physiol. 230, 1–6. https://doi.org/10.1016/j.cbpa.2018.12.008.

Hvas, M., Morin, A., Johansen, I.B., Vågseth, T., 2025. Acute stress-induced mortality in big Atlantic salmon at high temperatures is associated with insufficient oxygen uptake capacity. J. Therm. Biol. 132, 104231. https://doi.org/10.1016/j.jtherbio.2025.104231.

Hyde, D.A., Perry, S.F., 1987. Acid-base and ionic regulation in the American eel (*Anguilla Rostrata*) during and after prolonged aerial exposure: branchial and renal adjustments. J. Exp. Biol. 133, 429–447.

Inokuchi, M., Hiroi, J., Kaneko, T., 2022. Why can Mozambique tilapia acclimate to both freshwater and seawater? Insights from the plasticity of ionocyte functions in the euryhaline teleost. Front. Physiol. 13, 2022.

Jian, C.-Y., Cheng, S.-Y., Chen, J.-C., 2003. Temperature and salinity tolerances of yellowfin sea bream, *Acanthopagrus latus*, at different salinity and temperature levels. Aquac. Res. 34 (2), 175–185. https://doi.org/10.1046/j.1365-2109.2003.00800.x.

Karnaky, K.J., 1986. Structure and function of the chloride cell of *Fundulus heteroclitus* and other teleosts. Am. Zool. 26, 209–224.

Kochhann, D., Sarmento, C.G., de Oliveira, J.C., Queiroz, H.L., Val, A.L., Chapman, L.J., 2021. Take time to look at the fish: behavioral response to acute thermal challenge in two Amazonian cichlids. J. Exp. Zool. Part A: Ecological and Integrative Physiology 335 (9–10), 735–744. https://doi.org/10.1002/jez.2541.

Kraskura, K., Hardison, E.A., Eliason, E.J., 2023. Body size and temperature affect metabolic and cardiac thermal tolerance in fish. Sci. Rep. 13 (1), 17900. https://doi.org/10.1038/s41598-023-44574-w.

Kwak, S.G., Kim, J.H., 2017. Central limit theorem: the cornerstone of modern statistics. Korean J. Anesthesiol. 70 (2), 144–156. https://doi.org/10.4097/kjae.2017.70.2.144.

Laurent, P., Chevalier, C., Wood, C.M., 2006. Appearance of cuboidal cells in relation to salinity in gills of *Fundulus heteroclitus*, a species exhibiting branchial Na^+ but not cl^- uptake in freshwater. Cell Tissue Res. 325, 481–492. https://doi.org/10.1007/s00441-006-0187-3.

Leung, J.Y.S., Zhang, S., Connell, S.D., 2022. Is ocean acidification really a threat to marine calcifiers? A systematic review and meta-analysis of 980+ studies spanning two decades. Small 18 (35), 2107407. https://doi.org/10.1002/smll.202107407.

Madeira, D., Narciso, L., Cabral, H.N., Vinagre, C., Diniz, M.S., 2013. Influence of temperature in thermal and oxidative stress responses in estuarine fish. Comp. Biochem. Physiol. Mol. Integr. Physiol. 166 (2), 237–243. https://doi.org/10.1016/J.CBPA.2013.06.008.

Mancera, J.M., McCormick, S.D., 2000. Rapid activation of gill Na^+,K^+-ATPase in the euryhaline teleost *Fundulus heteroclitus*. J. Exp. Zool. 287 (4), 263–274. https://doi.org/10.1002/1097-010X(20000901)287:4<263:AID-JEZ1>3.0.CO;2-I.

Marshall, W.S., Emberley, T.R., Singer, T.D., Bryson, S.E., McCormick, S.D., 1999. Time course of salinity adaptation in a strongly euryhaline estuarine teleost, *Fundulus heteroclitus*: a multivariable approach. J. Exp. Biol. 202 (11), 1535–1544. https://doi.org/10.1242/jeb.202.11.1535.

Marshall, W.S., Grosell, M., 2006. Ion osmoregulation , and acid – Base balance. Physiol. Fish. 177–230.

Mayer-Gostan, N., Naon, R., 1992. Effects of ambient ion concentrations on gill ATPases in fresh water eel, *Anguilla Anguilla*. Fish Physiol. Biochem. 10 (1), 75–89. https://doi.org/10.1007/BF00004656.

McCormick, S.D., 1993. Methods for nonlethal gill biopsy and measurement of Na^+, K^+-ATPase activity. Can. J. Fish. Aquat. Sci. 50 (3), 656–658. https://doi.org/10.1139/f93-075.

McCormick, S.D., Naiman, R.J., 1984. Osmoregulation in the brook trout, *Salvelinus fontinalis*—Ii. Effects of size, age and photoperiod on seawater survival and ionic regulation. Comp. Biochem. Physiol. Physiol. 79 (1), 17–28. https://doi.org/10.1016/0300-9629(84)90704-7.

Metzger, D.C.H., Healy, T.M., Schulte, P.M., 2016. Conserved effects of salinity acclimation on thermal tolerance and hsp70 expression in divergent populations of threespine stickleback (*Gasterosteus aculeatus*). J. Comp. Physiol. B 186 (7), 879–889. https://doi.org/10.1007/s00360-016-0998-9.

Mommsen, T.P., Vijayan, M.M., Moon, T.W., 1999. Cortisol in teleosts: dynamics, mechanisms of action, and metabolic regulation. Rev. Fish Biol. Fish. 9 (3), 211–268. https://doi.org/10.1023/A:1008924418720.

Monette, M.Y., Pancurak, S., Breves, J.P., 2025. Thermal tolerance plasticity of *Fundulus heteroclitus* is maintained in freshwater and fluctuating temperature conditions. J. Comp. Physiol. B. https://doi.org/10.1007/s00360-025-01633-0.

Moorman, B.P., Lerner, D.T., Grau, E.G., Seale, A.P., 2015. The effects of acute salinity challenges on osmoregulation in Mozambique tilapia reared in a tidally changing salinity. J. Exp. Biol. 218 (5), 731–739. https://doi.org/10.1242/jeb.112664.

Morgenroth, D., et al., 2019. Hemodynamic responses to warming in euryhaline rainbow trout: implications of the osmo-respiratory compromise. J. Exp. Biol. 222, jeb207522.

Morgenroth, D., et al., 2022. Kingfish (*Seriola lalandi*) adjust to low salinity with only subtle effects to cardiorespiratory and growth performance. Aquaculture 556, 738268.

Morim, T., Bigg, G.R., Madeira, P.M., Palma, J., Duvernell, D.D., Gisbert, E., Cunha, R.L., Castilho, R., 2019. Invasion genetics of the mummichog (*Fundulus heteroclitus*): recent anthropogenic introduction in Iberia. PeerJ 7, e6155. https://doi.org/10.7717/peerj.6155.

Motulsky, H.M., Brown, R.E., 2006. Detecting outliers when fitting data with nonlinear regression – a new method based on robust nonlinear regression and the false discovery rate. BMC Bioinf. 7, 123.

Mugwanya, M., Dawood, M.A.O., Kimera, F., Sewilam, H., 2022. Anthropogenic temperature fluctuations and their effect on aquaculture: a comprehensive review. Aquacult. Fish. 7 (3), 223–243. https://doi.org/10.1016/J.AAF.2021.12.005.

Murchie, K.J., Cooke, S.J., Danylchuk, A.J., Danylchuk, S.E., Goldberg, T.L., Suski, C.D., Philipp, D.P., 2011. Thermal biology of bonefish (*Albula vulpes*) in Bahamian coastal waters and tidal creeks: an integrated laboratory and field study. J. Therm. Biol. 36 (1), 38–48. https://doi.org/10.1016/J.JTHERBIO.2010.10.005.

Nakamura, M., Watanabe, S., Kaneko, T., Masuda, R., Tsukamoto, K., Otake, T., 2020. Limited adaptation to non-natal osmotic environments at high water temperature in euryhaline wanderer fishes. Environ. Biol. Fish. 103 (2), 137–145. https://doi.org/10.1007/s10641-019-00940-0.

Parry, G., 1958. Size and osmoregulation in salmonid fishes. Nature 181 (4617), 1218–1219. https://doi.org/10.1038/1811218a0.

Pfeiler, E., Kirschner, L.B., 1972. Studies on gill ATPase of rainbow trout (*Salmo gairdneri*). Biochim. Biophys. Acta Biomembr. 282 (C), 301–310. https://doi.org/10.1016/0005-2736(72)90336-7.

Pörtner, H.-O., 2014. How and how not to investigate the oxygen and capacity limitation of thermal tolerance (OCLTT) and aerobic scope – remarks on the article by Gräns et al. J. Exp. Biol. 217 (24), 4432–4433. https://doi.org/10.1242/jeb.114181.

Pörtner, H.-O., Bock, C., Mark, F.C., 2017. Oxygen- and capacity-limited thermal tolerance: bridging ecology and physiology. J. Exp. Biol. 220 (15), 2685–2696. https://doi.org/10.1242/jeb.134585.

Röthig, T., Trevathan-Tackett, S.M., Voolstra, C.R., Ross, C., Chaffron, S., Durack, P.J., Warmuth, L.M., Sweet, M., 2023. Human-induced salinity changes impact marine organisms and ecosystems. Glob. Change Biol. 29 (17), 4731–4749. https://doi.org/10.1111/gcb.16859.

Ruhr, I.M., et al., 2020. Is aquaporin-3 involved in water-permeability changes in the killifish during hypoxia and normoxic recovery, in freshwater or seawater? J. Exp. Zool. A Ecol. Integr. Physiol. 333, 511–525.

Sandersfeld, T., Davison, W., Lamare, M.D., Knust, R., Richter, C., 2015. Elevated temperature causes metabolic trade-offs at the whole-organism level in the Antarctic fish *Trematomus bernacchii*. J. Exp. Biol. 218 (15), 2373–2381. https://doi.org/10.1242/jeb.122804.

Sandersfeld, T., Mark, F.C., Knust, R., 2017. Temperature-dependent metabolism in Antarctic fish: do habitat temperature conditions affect thermal tolerance ranges? Polar Biol. 40 (1), 141–149. https://doi.org/10.1007/s00300-016-1934-x.

Sardella, B.A., Kültz, D., Cech, J.J., Brauner, C.J., 2008a. Salinity-dependent changes in Na^+/K^+-ATPase content of mitochondria-rich cells contribute to differences in thermal tolerance of Mozambique tilapia. J. Comp. Physiol. B 178 (3), 249–256. https://doi.org/10.1007/s00360-007-0211-2.

Sardella, B.A., Kültz, D., Cech, J.J., Brauner, C.J., 2008b. Salinity-dependent changes in Na+/K+-ATPase content of mitochondria-rich cells contribute to differences in thermal tolerance of Mozambique tilapia. J. Comp. Physiol. B 178 (3), 249–256. https://doi.org/10.1007/s00360-007-0211-2.

Sardella, B.A., Sanmarti, E., Kültz, D., 2008. The acute temperature tolerance of green sturgeon (*Acipenser medirostris*) and the effect of environmental salinity. J. Exp. Zool. Part A: Ecological Genetics and Physiology 309A (8), 477–483. https://doi.org/10.1002/jez.477.

Schreck, C.B., Tort, L., 2016. The concept of stress in fish. Fish Physiol. 35, 1–34. https://doi.org/10.1016/B978-0-12-802728-8.00001-1.

Schultz, E.T., McCormick, S.D., 2012. Euryhalinity in an evolutionary context. Fish Physiol. 32, 477–533. https://doi.org/10.1016/B978-0-12-396951-4.00010-4.

Shaughnessy, C.A., McCormick, S.D., 2018. Reduced thermal tolerance during salinity acclimation in brook trout (*Salvelinus fontinalis*) can be rescued by prior treatment with cortisol. J. Exp. Biol. 221 (6). https://doi.org/10.1242/jeb.169557.

Stewart, E.M.C., Frasca, V.R., Wilson, C.C., Raby, G.D., 2023. Short-term acclimation dynamics in a coldwater fish. J. Therm. Biol. 112, 103482. https://doi.org/10.1016/J.JTHERBIO.2023.103482.

Styga, J.M., Pienaar, J., Scott, P.A., Earley, R.L., 2019. Does body shape in fundulus adapt to variation in habitat salinity? Front. Physiol. 10–2019. https://doi.org/10.3389/fphys.2019.01400.

Todgham, A.E., Schulte, P.M., Iwama, G.K., 2005. Cross-tolerance in the tidepool sculpin: the role of heat shock proteins. Physiol. Biochem. Zool. 78 (2), 133–144. https://doi.org/10.1086/425205.

Tsuchida, S., 1995. The relationship between upper temperature tolerance and final preferendum of Japanese marine fish. J. Therm. Biol. 20 (1–2), 35–41. https://doi.org/10.1016/0306-4565(94)00024-D.

Vargas-Chacoff, L., Arjona, F.J., Polakof, S., del Río, M.P.M., Soengas, J.L., Mancera, J. M., 2009. Interactive effects of environmental salinity and temperature on metabolic responses of gilthead sea bream *Sparus aurata*. Comp. Biochem. Physiol. Mol. Integr. Physiol. 154 (3), 417–424. https://doi.org/10.1016/J.CBPA.2009.07.015.

Vargas-Chacoff, L., Arjona, F.J., Ruiz-Jarabo, I., García-Lopez, A., Flik, G., Mancera, J.M., 2020. Water temperature affects osmoregulatory responses in gilthead sea bream (*Sparus aurata* L.). J. Therm. Biol. 88, 102526. https://doi.org/10.1016/J.JTHERBIO.2020.102526.

Vargas-Chacoff, L., Regish, A.M., Weinstock, A., McCormick, S.D., 2018. Effects of elevated temperature on osmoregulation and stress responses in Atlantic salmon *Salmo salar* smolts in fresh water and seawater. J. Fish. Biol. 93 (3), 550–559. https://doi.org/10.1111/jfb.13683.

Venegas, R.M., Acevedo, J., Treml, E.A., 2023. Three decades of ocean warming impacts on marine ecosystems: a review and perspective. Deep Sea Res. Part II Top. Stud. Oceanogr. 212, 105318. https://doi.org/10.1016/J.DSR2.2023.105318.

Ventrella, V., Trombetti, F., Pagliarani, A., Trigari, G., Pirini, M., Borgatti, A.R., 1992. Salinity dependence of the ouabain-insensitive Mg^{2+}-dependent Na+-ATPase in gills of rainbow trout (*Oncorhynchus mykiss* Walbaum) adapted to fresh and brackish water. Comp. Biochem. Physiol. Part B: Comparative Biochemistry 101 (1–2), 1–7. https://doi.org/10.1016/0305-0491(92)90149-L.

Verberk, W.C.E.P., Henry, E., Leiva, F.P., Barbarossa, V., Schipper, A.M., 2026. Heat tolerance and its plasticity in freshwater and marine fishes reflect exposure to extremes and seasonal variation in habitat temperatures. Ecol. Lett. 29 (3), e70341. https://doi.org/10.1111/ele.70341.

Verberk, W.C.E.P., Sandker, J.F., van de Pol, I.L.E., Urbina, M.A., Wilson, R.W., McKenzie, D.J., Leiva, F.P., 2022. Body mass and cell size shape the tolerance of fishes to low oxygen in a temperature-dependent manner. Glob. Change Biol. 28, 5695–5707. https://doi.org/10.1111/gcb.16319.

Wendelaar Bonga, S.E., 1997. The stress response in fish. Physiol. Rev. 77 (3), 591–625. https://doi.org/10.1152/physrev.1997.77.3.591.

Wood, C.M., et al., 2019. The osmorespiratory compromise in the euryhaline killifish: water regulation during hypoxia. J. Exp. Biol. 222.

Wood, C.M., Marshall, W.S., 1994. Ion balance, acid-base regulation, and chloride cell function in the common killifish, *Fundulus heteroclitus*—a euryhaline estuarine teleost. Estuaries 17 (1), 34–52. https://doi.org/10.2307/1352333.

Zaragoza, O.D.R., Rodríguez, M.H., Bückle Ramirez, L.F., 2008. Thermal stress effect on tilapia *Oreochromis mossambicus* (Pisces: cichlidae) blood parameters. Mar. Freshw. Behav. Physiol. 41 (2), 79–89. https://doi.org/10.1080/10236240801896223.

Zhang, Y., Kieffer, J.D., 2014. Critical thermal maximum (CT_{max}) and hematology of shortnose sturgeons (*Acipenser brevirostrum*) acclimated to three temperatures. Can. J. Zool. 92 (3), 215–221. https://doi.org/10.1139/cjz-2013-0223.

Zimmer, A.M., Perry, S.F., 2022. Physiology and aquaculture: a review of ion and acid-base regulation by the gills of fishes. Fish Fish. 23, 874–898.